

Investigation on the Cytotoxicity and Apoptosis of Citrate Based Silver Nanoparticles, In Vitro

Laya Ebrahimi¹, PhD student;
Saeid Hosseinzadeh¹, PhD; Maryam
Pourmontaseri¹, PhD; Jafar Jalaei²,
PhD

¹Department of Food Hygiene and
Public Health, School of Veterinary
Medicine, Shiraz University, Shiraz,
Iran

²Department of Basic Sciences
School of Veterinary Medicine, Shiraz
University, Shiraz, Iran

Correspondence:

Saeid Hosseinzadeh, PhD;
Department of Food Hygiene and
Public Health, School of Veterinary
Medicine, Shiraz University, Shiraz,
Iran

Tel: +98 917 6018069

Email: hosseinzadeh@shirazu.ac.ir.

Received: 6 July 2018

Revised: 4 August 2018

Accepted: 8 September 2018

Abstract

Background: With the advancement of nanotechnology, nanoparticles have been applied in our modern society. However, the hazardous effects of nanoparticles on organisms have not been thoroughly clarified yet. Considering the migration of nanoparticles in food and its subsequent consumption by humans, we have employed normal cell line, the African green monkey kidney cell line (Vero) for evaluation of the cytotoxic activity of the silver nanoparticles. Currently, there are various approaches to perform toxicity tests. In this study, we investigated the effects of citrate-based silver nanoparticles on Vero cells to explore the adverse effects of these nanoparticles.

Methods: In an experimental work, to synthesize silver nanoparticles, silver nitrate and citric acid were used. Nanoparticles were further characterized by UV-Visible Spectroscopy, Dynamic Light scattering (DLS) and Scanning Electron Microscopy (SEM). Cells were exposed to various concentrations of the nanoparticles (1.56 to 1000 µg/ml) for 24 h and 48h. The cytotoxic activity and apoptosis were determined using MTT assay and acridine orange/ethidium bromide (AO/EB) staining, respectively.

Results: The present study showed a dose-dependent cytotoxicity of the silver nanoparticles with log IC₅₀ values of ~10.68 and 2.06 µg/ml for 24 h and 48 h, respectively on Vero cell lines. Analysis by AO/EB staining indicated that the silver nanoparticles induced apoptosis in the cell lines.

Conclusion: Silver nanoparticles revealed cytotoxic effects on the Vero cells which was associated with the method of synthesis of silver nanoparticles.

Please cite this article as: Ebrahimi L, Hosseinzadeh S, Pourmontaseri M, Jalaei J. Investigation on the Cytotoxicity and Apoptosis of Citrate Based Silver Nanoparticles, In Vitro. *J Health Sci Surveillance Sys*. 2018;6(4):190-197.

Keywords: Silver nanoparticles, Vero cells, Cytotoxicity, Apoptosis

Introduction

Nanoparticles are an emerging class of functional materials. Application fields for nanoparticles range from medical imaging and new drug delivery technologies to various industrial sections.¹ Numerous chemical and physical methods are used for synthesizing silver nanoparticles.² The highly accepted chemical approaches were employed to synthesize silver nanoparticles including physicochemical and chemical reduction, using a variety of inorganic and organic reducing agents, radiolysis and electrochemical techniques.³ Metallic nanoparticles,

such as gold or silver ones, are applied in many fields.⁴ Silver nanoparticles are interesting for their scientific and commercial applications as disinfectant, antimicrobial, biosensor materials, cosmetic products and electronic components. The silver nanoparticle rather than the weak antibacterial agents are involved in water disinfection, food packaging, and medical and textile industry. They might also be involved in neutralizing these adhesive substances, leading to inhibition of the biofilm formation.⁵ These nanoparticles are well-known substances used in the biomedical materials as antimicrobial compounds.⁴ They give rise to the destruction of the sulfur and

phosphorus compounds in proteins and DNA, leading to cell death.^{6,7} Due to their adverse effect on the microorganisms, such nanosized particles can be useful in preparing new wound dressings.⁸ Also, according to Castro-Mayorga, nanocomposites, on the basis of their stabilized silver nanoparticles, can be a substitute for the existing food packaging.⁹ The nanoparticles protect the foodstuff from undesirable microorganisms, hence improving their shelf life.⁷ Silver nanoparticles can be synthesized and stabilized in the presence of polymers.¹⁰⁻¹³ During the synthesis of the polyethylene food packaging, a certain amount of silver nanoparticles was also used. These nanoparticles can migrate from the packaging to the foodstuff which will be subsequently consumed by humans; therefore, evaluation of cytotoxic activity is an important area of research.¹⁴ Evidence shows that accumulating the nanoparticles differ significantly from traditional materials and may cause different toxicities.¹ Frey et al. (2017) investigated cytotoxic effect of silver nanoparticles on the 3T3 Cells (Healthy fibroblast cells).¹⁵

Hernández-Sierra et al. (2011) have reported that cytotoxicity of silver nanoparticles are prepared with sodium tetrahydroborate (less than 20 nm) on the human periodontal fibroblasts.¹⁶ Also, the cytotoxicity of green synthesis of AgNPs was studied using the *Artemisia tournefortiana* extract on the HT-29 and HEK293 cell lines.¹⁷

With the rapid development of nanotechnology and the pervasive use of nano-products, the risk of human exposure has rapidly increased, and reliable toxicity test systems are immediately needed.^{1,18} The cytotoxicity of citrate-based silver nanoparticles on the Vero cells has not been reported elsewhere.

In this study, we selected silver nanoparticles, which have been commonly used in the industry, as candidate toxicants. However, given the potency of the nanoparticles (as new packaging system) to migrate in the food stuff and its subsequent side effects, this study was designed to synthesize citrate-based silver nanoparticles and evaluate their potential toxicity in the African green monkey kidney (Vero) cell line.

Materials and Methods

Preparation of Silver Nanoparticles

Silver nitrate (1.7 g) and citric acid (4.2 g) were dissolved in 9.2 mL distilled water in separate well-cleaned dry beakers. Then, this solution was heated on a stirring hot plate at 250°C for 45 minutes in order to evaporate the water and formation of powder of silver nanoparticles.¹⁹

Characterization of Silver Nanoparticles *UV-Visible Spectroscopy*

The UV-vis spectra of the silver suspensions

were recorded using UV-1800 spectrometer over the wavelength ranging from 300 nm to 700 nm (Shimadzu, Japan).²⁰

Dynamic Light Scattering (DLS)

The hydrodynamic sizes and Zeta Potential (mV) were calculated by dynamic light scattering (DLS) (SZ- 100, Horiba, Japan).^{21,22}

Scanning Electron Microscope

The nanoparticle images are obtained in an electron scanning microscope (TESCAN, Czech Republic, Model-TESCAN-Vega 3, at the Department of the Central Laboratory of Shiraz University). The details regarding applied magnification, voltage used and the size of the nanoparticle of the image were implanted on the photographs itself.

Evaluation of Cytotoxicity

For determining the cytotoxicity caused by citrate based silver nanoparticles, MTT 3-(4,5 Dimethylthiazol-2-yl)-2,5 diphenyltetrazolium bromide assay, as a colorimetric assay, was employed to determine the cell metabolic activity. In this method, 3-(4,5-dimethyl-2-thiazolyl)-2,5-diphenyl-2H-tetrazolium bromide turns into azure formazan by the succinate dehydrogenase in living cells. Briefly, the Vero cells were plated onto 96-well flat bottom culture plates to be exposed to various concentrations of silver nanoparticles. All cultures were incubated for 24 h at 37 °C in a humidified incubator. After 24 h of incubation (37 °C, 5% CO₂ in a humid atmosphere), 10 µL of MTT solution (5mg/mL in PBS) was added to each well, and the plate was incubated for a further 4 h at 37 °C. The resulting formazan was dissolved in 100 µL of DMSO with gentle shaking at 37 °C, and absorbance was measured by means of colorimetric measurements. The results were given as the mean of three independent experiments. Results are finally related to the cellular toxicity.²²⁻²⁴ Cells were incubated with 1.56, 3.12, 6.25, 12.5, 25, 50, 100, 200, 400, 800 and 1000 µg/ml concentrations of silver nanoparticles.

Ethidium Bromide/Acridine Orange Double Staining Assay

Cells were cultured on a 6-well plate (2 ×10⁵ cells per well in 2 ml). After overnight growth, silver nanoparticles at the concentrations of 0, 50, 100, 200 and 400 µg/ml for Vero cells were added. The cells were incubated for 24 hours; then, the cells were washed with 0.1 M PBS, pH 7.4 and collected by centrifugation at 1200 RPM for 10min. They were resuspended in 25µl of dye mixture [100 µg/ml of acridine orange and 100µg/ml of ethidium bromide prepared in PBS and mixed gently]. 10µl of the preparations was placed on a microscope slide

and examined under 400 X magnification, using the epifluorescence and filter combination (CETI 040856).²⁵

Phase-Contrast Microscopy

Cell morphology was evaluated using a phase-contrast microscopy. Cells were cultured onto a 6-well plate (1.5×10^5 cells per well in 2 ml). After overnight growth, silver nanoparticles at the concentrations of 0 and 400 $\mu\text{g/ml}$ for Vero cells were added.¹

Scanning Electron Microscope

Cell morphology was also investigated by a scanning electron microscopy. After 2 days of cell seeding, they were rinsed with PBS and fixed with 3% of glutaraldehyde for 2 hours at 4°C. They were dehydrated with concentrations of 50%, 60%, 70%, 80%, 90%, and 100% v/v of ethanol every 30 minutes and dried under a fume hood. Finally, the SEM analysis was used to observe the morphology with Scanning Electron Microscope.²⁶

Statistical Analysis

All data were represented as the mean \pm SD of three independent experiments. The statistical differences

between MTT and EB/AO tests were analyzed by one-way ANOVA and independent sample t-test using SPSS19. P values <0.05 were considered statistically significant. A minimum of 100 cells were counted in each assay. The IC₅₀ was calculated by nonlinear regression analysis using GraphPad Prism v.6.0 software (GraphPad Prism, USA).

Results

Synthesis of Silver Nanoparticles

Aqueous silver colloids were prepared by reduction of Silver nitrate with citric acid. After a few minutes, the suspension turned yellow (Figure 1a).

UV-Visible Spectroscopy Analysis

UV-Vis spectra of silver nanoparticle solution treated at different temperatures are shown in Figure 1. As seen in this Figure, adsorption band at 425 nm was observed on the spectra of the as-synthesized solution and solution treated at 100 °C (Figure 1b).

Particle Size and Zeta Potential Determination (DLS)

The average particle size of nanoparticles was 49.2 nm (Figure 1). The values of zeta potential in the

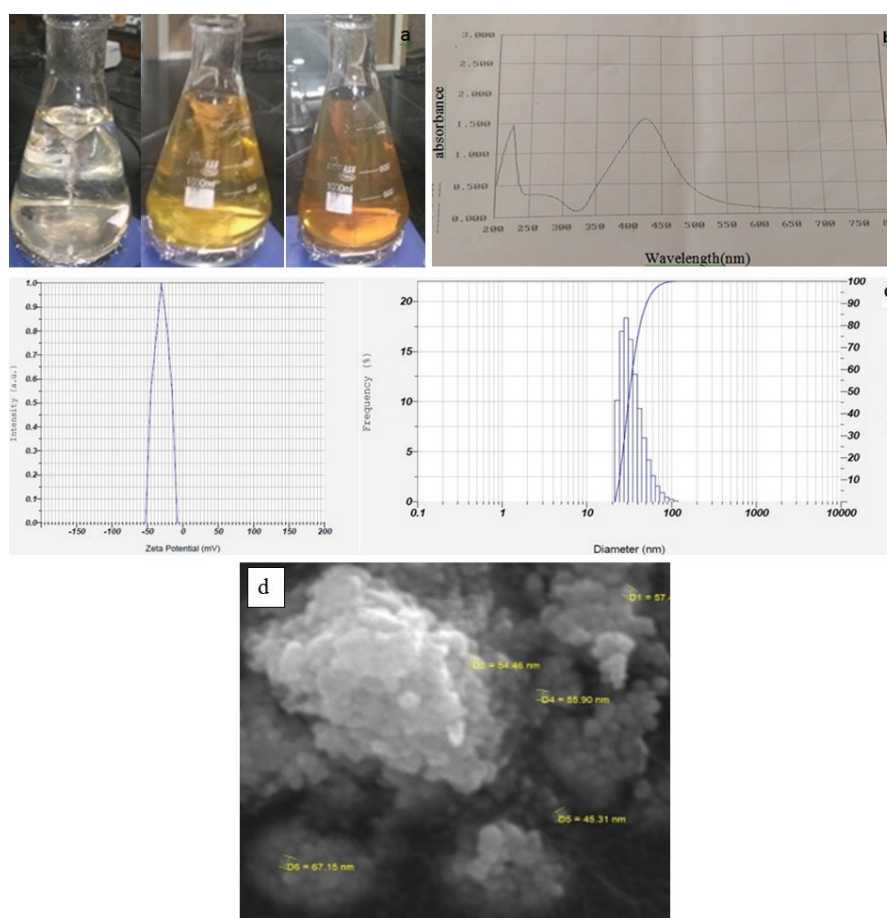


Figure 1: a Synthesis of silver nanoparticles, color change at 45 min into brown; b Characterization of silver nanoparticles by UV-Visible Spectroscopy ; c Measurement of the hydrodynamic Zeta Potential and sizes of silver nanoparticles by dynamic light scattering (DLS); and d Scanning electron micrograph of silver nanoparticles.

peak was determined -30 mV (Figure 1c).

Scanning Electron Microscopy Studies

Size and Morphology Analysis of silver nanoparticles was performed by Scanning Electron Microscopy (SEM). Details of the images are shown in Figure 1.d, showing the particles which are more or less spherical. The SEM analysis revealed that the particle size of silver nanoparticles was about <100 nm.

Evaluation of cytotoxicity

The effect of silver nanoparticles in the Vero cells, assessed by MTT assay, are shown in Figure 2 and Table 1. It was shown that cytotoxicity of the nanoparticles was a dose- and time-dependent mechanism. The cytotoxicity at the highest concentration of the nanoparticles was 67.53 and 68.54, while at the lowest concentration these values were 20.096 and 25.51 at 24 h and 48 h, respectively ($P < 0.05$).

Log concentration IC_{50} values were about 10.68 $\mu\text{g}/\text{ml}$ and 2.06 $\mu\text{g}/\text{ml}$ after 24 h and 48h of exposure with

silver nanoparticles, respectively (Figure 3).

Ethidium Bromide/Acridine Orange Double Staining Assay

As shown in Figures 4 and 5, cells exhibited different colors under the fluorescence microscope, in which the viable cells were recognized by bright green nuclei with intact cell membranes; early apoptotic cells were marked by nuclear condensation of chromatin as fragments and late apoptotic cells contained condensed chromatin and showed orange appearance. The necrotic cells are defined by the intact structures and orange nucleus.

The percentage of viable cells at the concentrations of 0, 50, 100, 200 and 400 $\mu\text{g}/\text{ml}$ were 85.53, 54.36, 53.44, 49.38, 33.82, respectively ($P < 0.05$) (Table 2).

Phase-Contrast Microscopy

After 24 hours of the treatment, the changes in cell morphology were examined using phase-contrast microscopy. Morphological changes included (Figure 6) few cellular extensions and increased the floating cells.

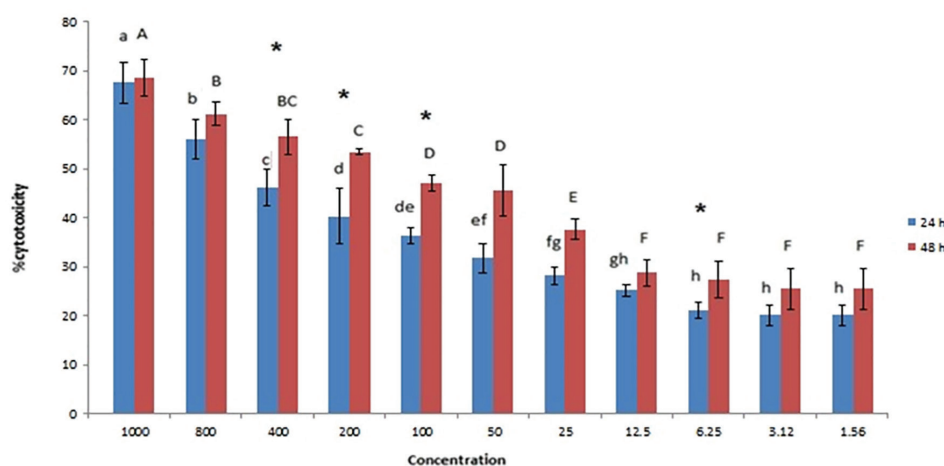


Figure 2: Cell cytotoxicity was measured using the MTT assays

Table 1: Cell cytotoxicity measured using the MTT assays

Concentration ($\mu\text{g}/\text{ml}$)	Cytotoxicity 24 h (%)	Cytotoxicity 48 h (%)
1000	67.5333 \pm 1.45204 ^a	68.5433 \pm 0.73711 ^A
800	56.0733 \pm 4.16997 ^b	61.2033 \pm 3.82321 ^B
400	46.1267 \pm 3.93612 ^{c*}	56.5333 \pm 2.33635 ^{BC*}
200	40.36 \pm 3.67759 ^{d*}	53.47 \pm 3.59626 ^{C*}
100	36.21 \pm 5.71488 ^{de*}	47.0933 \pm 0.68973 ^{D*}
50	31.73 \pm 1.65145 ^{ef}	45.6867 \pm 1.64385 ^D
25	28.1367 \pm 3.08845 ^{fg}	37.6267 \pm 5.27305 ^E
12.5	25.2067 \pm 1.92931 ^{gh}	28.8467 \pm 2.15175 ^F
6.25	21.0067 \pm 1.25803 ^{h*}	27.3233 \pm 2.71929 ^{F*}
3.12	20.0967 \pm 1.66236 ^h	25.5133 \pm 3.68838 ^F
1.56	20.0967 \pm 1.66236 ^h	25.5133 \pm 3.68838 ^F

Different letters in each column show significant difference ($p < 0.05$).

*Shows significant difference between each the columns ($p < 0.05$).

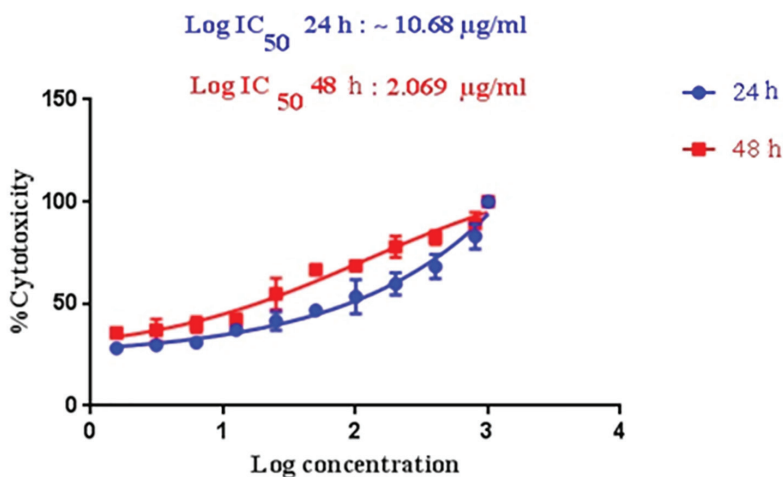


Figure 3: IC₅₀ of silver nanoparticles on the Vero cells

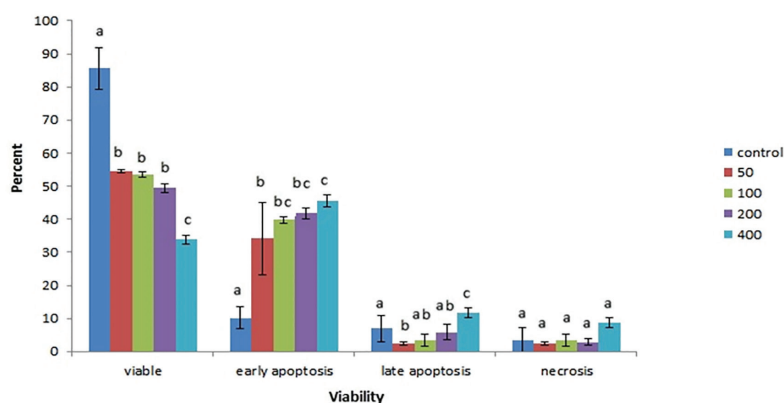


Figure 4: Cells w observed by fluorescence microscopy

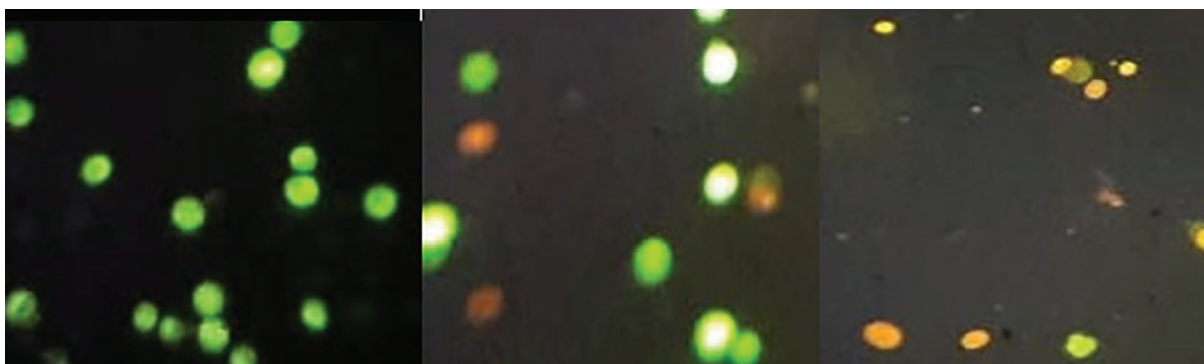


Figure 5: The green c and red colors indicate the fluorescence of detected live cells and dead cells, respectively

SEM Analysis

The alteration in the morphology of Vero cells treated with silver nanoparticles was observed under scanning electron microscope. Vero cells treated with silver nanoparticles displayed typical morphological features of necrosis. Control Vero cells showed their normal shape and surface morphology (Figure 7). The honeycomb shaped cells were observed after 24 hours of commencing the treatments. The necrotic type cell was confirmed by loss of membrane and formation of pores.

Discussion

The increasing use of nanomaterials in consumer and industrial products has aroused global concern regarding their toxicity and their fate in the biological systems. While the toxicity of many bulk materials is well understood, it is not known at what concentration or size they begin to exhibit new toxicological properties due to nanoscopic dimensions.¹ In the present study, we aimed to evaluate the cytotoxic activity of the silver nanoparticles on non-cancerous Vero cell lines.

Table 2: Cells observed by fluorescence microscopy

Concentration ($\mu\text{g/ml}$)	Viable	Early apoptosis	Late apoptosis	Necrosis
Control (0 $\mu\text{g/ml}$)	85.53 \pm 6.15997 ^a	10.1867 \pm 3.27234 ^a	6.9333 \pm 3.88039 ^a	3.5067 \pm 3.71512 ^a
50	54.3672 \pm 0.48301 ^b	34.1809 \pm 11.00199 ^b	2.3513 \pm 0.50006 ^b	2.3313 \pm 0.46599 ^a
100	53.4492 \pm 0.88324 ^b	39.7591 \pm 1.00692 ^{bc}	3.4492 \pm 1.75742 ^{ab}	3.4492 \pm 1.77786 ^a
200	49.3887 \pm 1.44023 ^b	41.8672 \pm 1.66096 ^{bc}	5.8356 \pm 2.39996 ^{ab}	2.9085 \pm 0.88935 ^a
400	33.8204 \pm 1.29079 ^c	45.5996 \pm 1.91449 ^c	11.7577 \pm 1.40131 ^c	8.8156 \pm 1.41989 ^a

Different letters in each column show significant difference ($p < 0.05$).

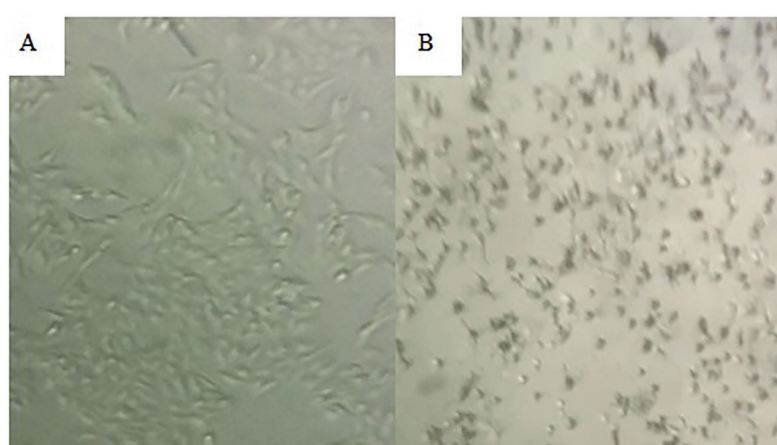


Figure 6: Effects of silver nanoparticles on cellular morphology. Image of Vero cells (A(0 $\mu\text{g/ml}$) and B(400 $\mu\text{g/ml}$)) were observed by phase-contrast microscopy (10 \times).

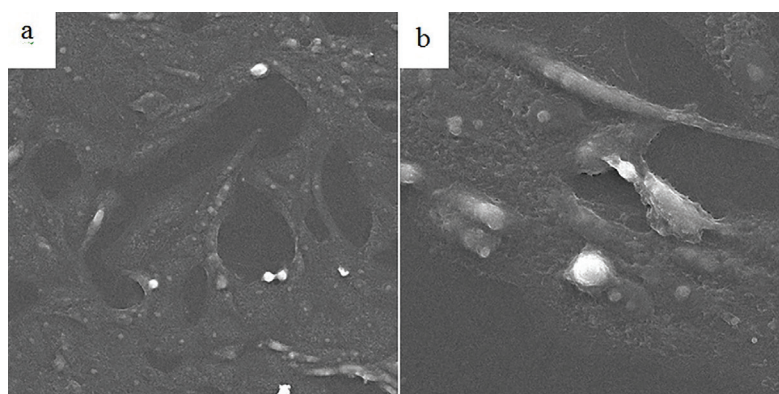


Figure 7: Scanning electron micrograph of the cells. Image of Vero cells (a(0 $\mu\text{g/ml}$) and b(400 $\mu\text{g/ml}$)).

Our results showed dose- and time-dependent cytotoxic activity on Vero cells, following 24 h and 48 h of the exposure which was gradually increased.

Frey et al. (2017) found a high cytotoxic effect of silver nanoparticles (40 nm) on 3T3 Cells (Healthy fibroblast cells). The viability of the cells in the concentration of 5-10 $\mu\text{g/ml}$ of silver nanoparticles on the 3T3 cells reduced to zero.¹⁵ Their results were in the same line with our findings.

Hernandez-Sierra (2011) evaluated 3 silver

nitrate nanoparticles that were prepared with sodium tetrahydroborate, solutions ≤ 10 , 15–20, and 80–100 nanometers in diameter at different concentrations and exposure times to induce cytotoxic effects in the healthy human periodontal tissue fibroblast cell primary cultures. However, no apparent cytotoxic effect on the human periodontal fibroblastic cells was observed by the 80-100 nm particles (24, 72 168 h); however, there was an increase in the cell viability.¹⁶ The results were different from our findings which was possibly due to the method of synthesis of

nanoparticles and/or type of the cells.

According to the results of the Movagharnia et al. (2018), the green fabricated AgNPs revealed a more cytotoxic effect on the HT-29 ($IC_{50}=40.71$ mg/mL) compared to the normal cells (Human embryonic kidney 293, HEK293) ($IC_{50}=61.38$ mg/mL). Moreover, the green synthesis of AgNPs was conducted using the *Artemisia tournefortiana* extract.¹⁷

Other studies on the synthesized silver nanoparticles (43 nm) by Marine algae (seaweeds) (Saraniya et al. 2011) revealed the toxic effects against Hep-2, MCF-7, and HT-29. The nanoparticles showed a mild cytotoxic potency against MCF-7 and HT-29 cell lines, but more strongly against Hep2 cells and less so against the normal Vero cell line. Cytotoxicity of nanoparticles was dependent on the differences in morphology of the cell membranes.²⁷

It seems that the biological production of nanoparticles using these plant extracts is can enhance their medicinal effects, and has a lesser toxic impact on the healthy cells.

It was found in our study that the toxicity of various sizes of the synthesized citrate-based silver nanoparticles on the Vero cells was different from what was previously reported in other studies. In order to evaluate the cytotoxicity, we employed different concentrations of the nanoparticles in two different times here. It is, therefore, suggested that researchers should work on a few more cells, especially the normal intestinal cell lines. Synthesis of various green nanoparticles is also suggested as safer nanomaterials used in the modern food packaging.

The use of silver nanoparticles for food packaging will surely emerge as one of the novel approaches in the future. Thus, the method of synthesis is an important factor in reducing the damage to the healthy cells and destroying the cancerous cells.

Conclusion

The present results showed that citrate-based silver nanoparticles exerted toxic effects, *in vitro*. Therefore, it is not suitable for food packaging, whereas the biosynthesized methods to synthesize such nanoparticles are more appropriate for use in the modern food packaging system.

Acknowledgement

Authors would like to thank Miss Aghazi and Mrs. Younesian at the Department of Food Hygiene and Public Health and Mrs. Masoodian, Mr. Mahboobi and Mr. Jaberri at the Central Laboratory for their invaluable support. The work was financially supported by Shiraz University, Shiraz, Iran.

Conflict of Interest: None declared.

References

- Lee Y-H, Cheng F-Y, Chiu H-W, Tsai J-C, Fang C-Y, Chen C-W, et al. Cytotoxicity, oxidative stress, apoptosis and the autophagic effects of silver nanoparticles in mouse embryonic fibroblasts. *Biomaterials* 2014; 35(16): 4706-15 . <https://doi.org/10.1016/j.biomaterials.2014.02.021>.
- Senapati S. Biosynthesis and immobilization of nanoparticles and their applications, Thesis (PhD). University of Pune. India. 1 (2005).
- Verma P, Maheshwari SK. Minimum biofilm eradication concentration (MBEC) assay of Silver and Selenium nanoparticles against biofilm forming *Staphylococcus aureus*. *JMSCR* 2017; 5(4): 20213-20222. <https://dx.doi.org/10.18535/jmscr/v5i4.77>.
- Kumar S, Mitra A, Halder D. Centella asiatica leaf mediated synthesis of silver nanocolloid and its application as filler in gelatin based antimicrobial nanocomposite film. *LWT – Food Sci Technol* 2017; 75: 293-300. <https://doi.org/10.1016/j.lwt.2016.06.061>.
- Verma P. A review on synthesis and their antibacterial activity of Silver and Selenium nanoparticles against biofilm forming *Staphylococcus aureus*. *World J Pharm Pharmaceut Sci* 2015; 4: 652-77.
- Sotiriou GA, Pratsinis SE. Engineering nanosilver as an antibacterial, biosensor and bioimaging material. *Curr Opin Chem Biol* 2011; 1(1): 3-10. <https://doi.org/10.1016/j.coche.2011.07.001>.
- Eslami M, Bayat M, Nejad ASM, Sabokbar A, Anvar AA. Effect of polymer/nanosilver composite packaging on long-term microbiological status of Iranian saffron (*Crocus sativus* L.). *Saudi J Bio Sci* 2016; 23(3): 341-7. <https://doi.org/10.1016/j.sjbs.2015.07.004>.
- Bumbudsanpharoke N, Choi J, Ko S. Applications of nanomaterials in food packaging. *J Nanosci Nanotechnol* 2015; 15(9): 6357-72. <https://doi.org/10.1166/jnn.2015.10847> .
- Castro-Mayorga J, Fabra M, Lagaron J. Stabilized nanosilver based antimicrobial poly (3-hydroxybutyrate-co-3-hydroxyvalerate) nanocomposites of interest in active food packaging. *Innov Food Sci Emerg Technol* 2016; 33: 524-33. <https://doi.org/10.1016/j.ifset.2015.10.019>.
- Huang H, Yang X. Synthesis of polysaccharide-stabilized gold and silver nanoparticles: a green method. *Carbohydr Res* 2004; 339(15): 2627-31. <https://doi.org/10.1016/j.carres.2004.08.005>.
- Wang H, Qiao X, Chen J, Ding S. Preparation of silver nanoparticles by chemical reduction method. *Colloids Surf A* 2005; (256): 111-115. <https://doi.org/10.1016/j.colsurfa.2004.12.058>.
- Long D, Wu G, Chen S. Preparation of oligochitosan stabilized silver nanoparticles by gamma irradiation. *Radiat Phys Chem*. 2007; 76(7): 1126-31. <https://doi.org/10.1016/j.radphyschem.2006.11.001>.

- 13 Zielińska A, Skwarek E, Zaleska A, Gazda M, Hupka J. Preparation of silver nanoparticles with controlled particle size. *Procedia Chem.* 2009; 1(2): 1560-6. <https://doi.org/10.1016/j.proche.2009.11.004>.
- 14 Bumbudsanpharoke N, Ko S. Nano-food packaging: an overview of market, migration research, and safety regulations. *J. Food Sci.* 2015; 80(5): R910-R23. <https://doi.org/10.1111/1750-3841.12861>.
- 15 Frey EC. Influence of Silver Nanoparticle Surface Charge on Cytotoxic Efficacy against Cancer Cells, Thesis (PhD). University of California. San Luis Obispo. 1(2017).
- 16 Hernández-Sierra JF, Galicia-Cruz O, Salinas-Acosta A, Ruíz F, Pierdant-Pérez M, Pozos-Guillén A. *In vitro* cytotoxicity of silver nanoparticles on human periodontal fibroblasts. *J Clin Pediatr Dent* 2011; 36(1): 37-42. <https://doi.org/10.17796/jcpd.36.1.d677647166398886>.
- 17 Movagharnia R, Baghbani-Arani F, Shandiz S, Ataollah S. Cytotoxicity effects of green synthesized silver nanoparticles on human colon cancer (HT29) cells. *J Kashan Univ Med Sci—Feyz* 2018; 22(1): 31-8. <http://feyz.kaums.ac.ir/article-1-3196-en.html>.
- 18 Oberdörster G, Maynard A, Donaldson K, Castranova V, Fitzpatrick J, Ausman K, et al. Principles for characterizing the potential human health effects from exposure to nanomaterials: elements of a screening strategy. *Part Fibre Toxicol* 2005; 2(1): 8. <https://doi.org/10.1186/1743-8977-2-8>.
- 19 Kamali M, Ghorashi SAA, Asadollahi MA. Controllable synthesis of silver nanoparticles using citrate as complexing agent: Characterization of nanoparticles and effect of pH on size and crystallinity. *Iran J Chem Chem Eng* 2012; 31(4): 21-8.
- 20 Oćwieja M, Barbasz A, Walas S, Roman M, Paluszkiwicz C. Physicochemical properties and cytotoxicity of cysteine-functionalized silver nanoparticles. *Colloid Surface B* 2017; 160: 429-37. <https://doi.org/10.1016/j.colsurfb.2017.09.042>.
- 21 Oćwieja M, Adamczyk Z. Controlled release of silver nanoparticles from monolayers deposited on PAH covered mica. *Langmuir* 2013; 29(11): 3546-55. <https://doi.org/10.1021/la304855k>.
- 22 Gurunathan S, Han JW, Eppakayala V, Jeyaraj M, Kim J-H. Cytotoxicity of biologically synthesized silver nanoparticles in MDA-MB-231 human breast cancer cells. *BioMed Res Int* 2013; 2013. <https://doi.org/10.1155/2013/535796>.
- 23 Poormontaseri M, Hosseinzadeh S, Shekarforoush SS, Kalantari T. The effects of probiotic *Bacillus subtilis* on the cytotoxicity of *Clostridium perfringens* type a in Caco-2 cell culture. *BMC Microbiol* 2017; 17(1): 150. <https://doi.org/10.1186/s12866-017-1051-1>.
- 24 Tyliczszak B, Drabczyk A, Kudłacik-Kramarczyk S, Bialik-Wąs K, Kijkowska R, Sobczak-Kupiec A. Preparation and cytotoxicity of chitosan-based hydrogels modified with silver nanoparticles. *Colloid Surface B* 2017; 160: 325-30. <https://doi.org/10.1016/j.colsurfb.2017.09.044>.
- 25 Ciniglia C, Pinto G, Sansone C, Pollio A. Acridine orange/Ethidium bromide double staining test: A simple in-vitro assay to detect apoptosis induced by phenolic compounds in plant cells. *Allelopathy J* (2010); 26: 301-308.
- 26 Saudi A, Rafienia M, Zargar Kharazi A, Salehi H, Zarrabi A, Karevan M. Design and fabrication of poly (glycerol sebacate)-based fibers for neural tissue engineering: Synthesis, electrospinning, and characterization. *Polym Advan Technol* 2019; 30(6): 1427-40. <https://doi.org/10.1002/pat.4575>.
- 27 Devi J, Bhimba B. Anticancer activity of silver nanoparticles synthesized by the seaweed *Ulva lactuca* *in vitro*. *Sci Rep* 2012; 1: 242. <http://dx.doi.org/10.4172/scientificreports.242>.